Synthesis and kinetic analysis of hydromagnesite with different morphologies by nesquehonite method

Yulian Wang*,[1,2], Wanzhong Yin*,[3], Chuang Li[1,2] & Zhigang Yuan[1]

[1]Collogy of Materials Science and Engineering, Shenyang Ligong University, Shenyang 110 159, China

[2] State Key Laboratory of Mineral Processing, Beijing 100 160, China

[3] School of Resources & Civil Engineering, Northeastern University, Shenyang 110 819, China

E-mail: wangyulian@slyu.edu.cn

Hydromagnesite with different morphologies has been synthesized using self-made nesquehonite whiskers as raw materials. The synthesized samples have been characterized by X-ray diffraction (XRD) and scanning electron microscopy (SEM). The results show that porous rod-like hydromagnesite are generated at 328~353K and in the pH value of 9.30+0.2, while irregular flower-like and flat layered ones are synthesized in the pH values of 10.0+0.05 and 11.0+0.05, respectively. The yield of hydromagnesite improved linearly with the increase of the temperatures and solution pH values. Porous rod-like hydromagneiste crystals with good crystalline and uniform morphology are obtained when the pyrolysis time is over 60 min. Furthermore, the apparent activation energy of phase transformation is calculated to be 3.4080 kJ/mol. According to the results, the experimental data can be well described by the kinetic model, suggesting that the phase transfer rate is dependent on the temperature.

The design, preparation, and application of micro-nano materials with special structures are widely noted[1, 2]. The form of particles and their properties are closely related, and different particle shapes and sizes sometimes give different particle properties even for the same substance[3-5]. In the field of inorganic powder materials, the research and development of highly functional materials have been performed for many years through the control of crystal phase and morphology[6-9]. In recent years, materials with suitable sizes and morphologies have attracted much more attentions due to the utilization for various types of functional application fields, such as filter material, pharmaceuticals, cosmetic manufacturing, optical and chemical devices[10,11].

Hydromagnesite ($4MgCO_3 \cdot Mg(OH)_2 \cdot 4H_2O$) as an important new type of magnesium chemical materials, is generally known to exist as polymorphic fine crystals[12-14]. Due to its lower thermal-decomposition temperature, hydromagnesite can be used as the carrier and precursor for other magnesium salt products[6,12]. During the thermal decomposition process, hydomagnesite will convert to non-burning magnesium oxide and release nonflammable gases by absorbing lots of heat[9]. Therefore, hydromagnesite is also a preferable flame retardant. Moreover, hydromagnesite is widely used in many fields such as pigments, food, pharmaceutical and daily necessities[15].

To our knowledge, the morphology and size of hydromagnesite would vary with the raw materials and preparation methods. Porous hydromagnesite microspheres with rosette-like morphology was synthesized using $MgCl_2$ and Na_2CO_3 or other carbonate as raw materials [6,16-18]. Micro-rod hydromagnesite with a surface of "house of cards" structure was prepared by the reaction of $Mg(NO_3)_2$ and Na_2CO_3 at 353.2K[19,20]. Tubular hydromagnesite with a "house of cards" structure was obtained by heating needle-like nesquehonite ($MgCO_3 \cdot 3H_2O$)[21]. Petaloid hydomagnesite microspheres were also synthesized under ultrasonic irradiation[22]. It was found that nesquehonite could be transformed to rod-like or tubular hydromagnesite by adjusting pH values and reaction temperature when the temperature was higher than 323K[23, 24]. Up to now, there are plenty of studies about the preparation of hydromagnesite. Hydromagnesite is mainly prepared by the direct precipitation method, which is to mix soluble

magnesium salt and carbonate salt under some conditions. However, direct precipitation method will result in a close packing "stack" structure constructed by nanosheets. While hydromagnesite with different morphology and high purity can be well obtained by indirect method, which is through rod-like nesuqehonite transformation. Overall, it is observed that those researches mainly focused on preparation instead of formation mechanism.

In this paper, porous rod-like, irregular flower-like and flat layered hydromagnesite were prepared using self-made rod-like nesquehonite whiskers as raw materials. More significantly, the technology mentioned above plays an important role in efficient mineral resources utilization. The influence of pyrolysis temperature, time, and pH values on the crystal structure and morphology were characterized by X-ray diffraction (XRD) and scanning electron microscopy (SEM). Moreover, phase transfer kinetics and morphology transition mechanism of hydromagnesite were analyzed in detail.

Experimental Section
Preparation of nesuqehonite whiskers

Nesquehonite whiskers were synthesized with magnesite method. Natural magnesite ($MgCO_3$, Dandong, China) was used as a raw material. The light MgO powders were obtained by calcining magnesite in a muffle furnace for 3.5 h at 1023K. Then the above MgO powders were crushed and screened. The diameter of the undersize light MgO was about 120 micrometer. According to the solid/liquid of 1:40 (mass ratio), the undersize light MgO was mixed with deionized water at 363K. Then the mixed solution was stirred at 333K in a thermostatic water bath. Thus magnesium hydroxide [$Mg(OH)_2$] slurry was obtained after a certain hydration time. Afterwards, CO_2 was blown into the resulting slurry at a rate of 0.16 $m^3 \cdot min^{-1}$ at 273K. A self-made cooling water system was used to maintain the reaction temperature at 273K. The reaction finished when the *p*H value was in the range of 7.00~8.00, and then the mixture was filtered with a vacuum filter. The obtained clear solution, which was magnesium bicarbonate [$Mg(HCO_3)_2$], was stirred for 1.0 h at 323K, and then filtered and dried. Thus, nesquehonite whiskers were obtained.

Preparation of hydromagnesite

Hydromagnesite were prepared via pyrolysis method using nesuqehonite whiskers as precursor reactants. All chemicals used were analytical grade (Tian-jin Kemiou Chemical Reagent Co., Ltd.). According to the solid/liquid of 1:30 (mass ratio), a certain amount of nesquehonite powders was mixed with deionized water. Then NaOH with a concentration of 5.0 $mol \cdot L^{-1}$ was added to adjust the *p*H value of the mixed solution, followed by stirring at room temperature to obtain the precursor solution. The *p*H value was measured by a digital *p*H meter (Phs-3C, Shanghai Leici Instrument Factory, China). The resultant precursor solution was stirred for 0~120 min at 328~353K, then filtered and dried. The white precipitates were obtained and subjected to analysis. The solution conductivity was recorded with conductivity measurer (DDSJ-308, Shanghai Leici Instrument Factory, China) during the pyrolysis process.

Characterization
Hydromagnesite yield measurement

The yield of hydromganesite was calculated according to [Eq. (1)].

$$\gamma = \frac{m_1}{m_2} \times 100\% \qquad \qquad \dots (1)$$

where, γ is defined as yield (%), m_1 is real production of hydrogmanesite (g), m_2 is theoretical yield of hydromagnesite. Theoretical yield of hydromagnesite, m_2, is usually determined in accordance with the transition reaction equation mentioned [Eq. (2)].

$$5[MgCO_3 \cdot 3H_2O] \rightarrow 4MgCO_3 \cdot Mg(OH)_2 \cdot 4H_2O + 10H_2O + CO_2 \uparrow \qquad \dots (2)$$
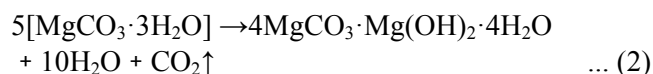
XRD and SEM study

The phase compositions of the products were analyzed by XRD (MPDDY2094, PAN alytical B.V., CuKα 7° $\cdot min^{-1}$). The wavelength was 1.54056Å, the stability of currency was ±0.03%, the accuracy of θ was ±0.002°, the tube voltage was 40kv, the tube current was 40mA, the rate of scanning was 7°/min and the scanning range was 2θ=10~90°. The morphologies of the products were examined by scanning electron microscopy (SEM, JSM-6360LV, Jeol Ltd.) at an accelerating voltage of 0.5-30.0 kV, a beam current of 1pA-1μA and a resolution of 1.0nm after the samples were coated with gold.

Results and Discussion

Effect of pyrolysis temperature

Figure 1(a) shows XRD patterns of products obtained at different temperatures. All peaks of the resultant products obtained at 328~343K belong to the monoclinic crystalline phase of hydromagnesite ($4MgCO_3 \cdot Mg(OH)_2 \cdot 4H_2O$). The smooth baseline, the narrow peak width, and the strong intensity of the peaks indicate that hydromagnesite is well crystallized. It is illustrated that nesquehonite was completely transformed into hydromagnesite in the temperature range, since nesquehonite peaks has not been found. That means the purity of hydromagnesite can be high. SEM images of hydromagnesite were presented in Fig.1(b)~Fig.1(e). It can be seen that hydromagnesite obtained at 328~353K is porous rod, the structure of which was formed by the superposition of nano sheets(Figs1(b), 1(c), 1(d), and 1(e)). There are cavities among the sheets, which leads to the formation of porous structure.
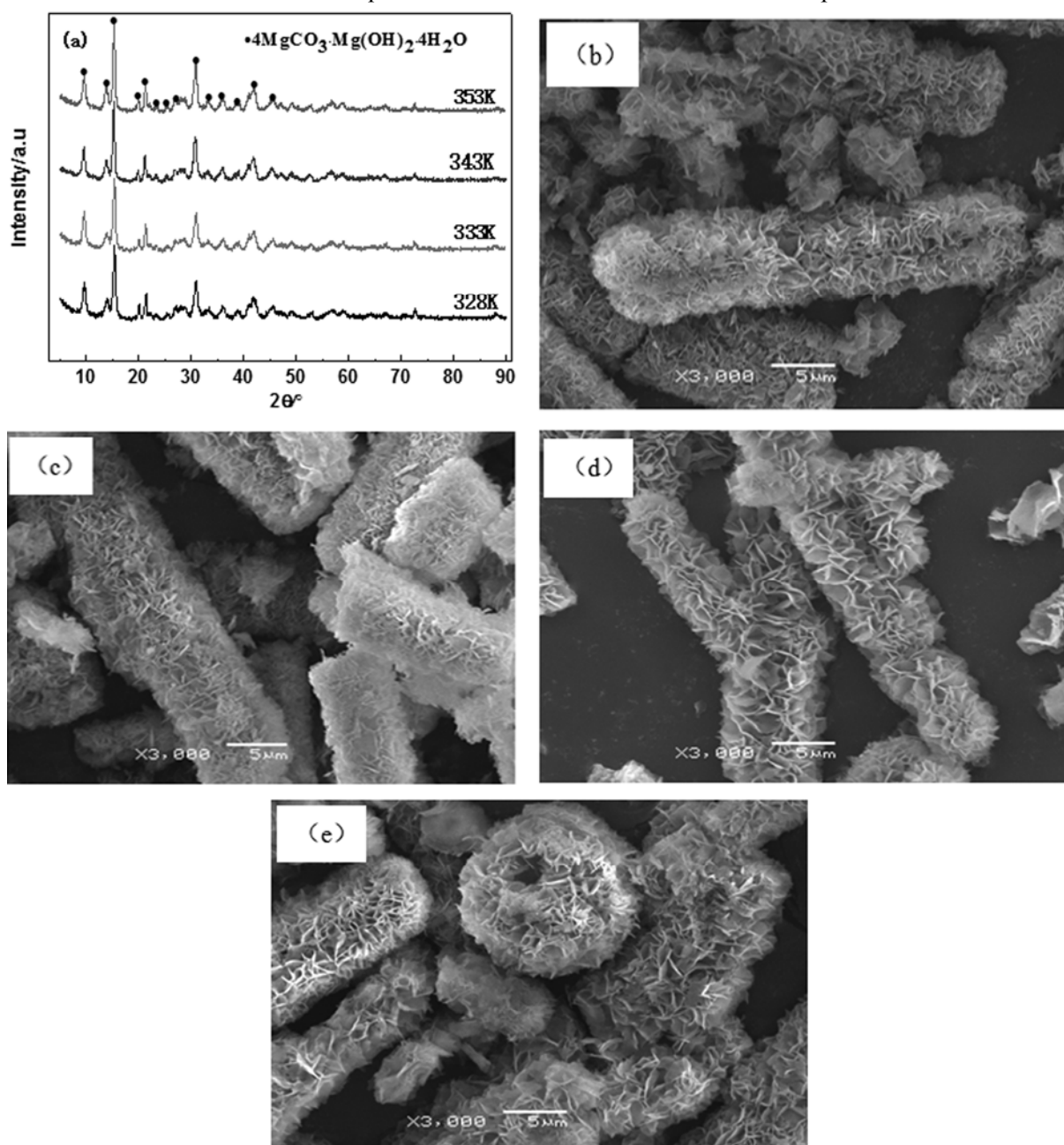

Fig. 1 — XRD patterns of products obtained at different temperatures (a) and SEM images of hydromagnesite obtained at (b) 328K; (c)333K; (d)343K and (e)353K.

According to Eq.(1)~(2), the yield of hydromagnesite obtained at different temperatures was calculated. The results are given in Table 1. It can be observed that the maximum of the yield was 89.06% at 343K, while the yield at 353K is lower than that at 343K. The possible reason may be that the water of the solution evaporates when the temperature is higher than 343K. It is obviously that

Table 1 — Yield of hydromagnesite obtained at different temperatures

Temperature	Results			
(K)	Mass of N, g	Theoreticla yield of H, g	Real production of H, g	Yield, %
328	10.03	6.77	4.69	69.27
333	10.02	6.76	5.40	79.88
343	10.03	6.77	6.03	89.06
353	20.01	13.51	11.41	84.4

(In table 1, N and H stands for nesquehonite and hydromagnesite, respectively. The meaning is the same in table 2.)

the yield of hydromagensite can be promoted by a higher pyrolysis temperature.

Influence of *p*H value of nesquehonite solution

Figure 2(a) represents the products obtained at different pH values of nesquehonite solutions. As shown in Fig. 2(a), products prepared in different *p*H values are well crystallized hydromagnesite with high purity. Hydromagnesite obtained at natural *p*H is porous rod-like microstructure (Fig. 2(b)). When the solution *p*H value increases to 10.0+0.05 and 11.0+0.05, hydromagnesite is irregular flower-like (Fig. 2(c)) and flat layered crystals (Fig. 2(d)), respectively. The flower structure is assembled from twisted two-dimensional nano sheets.

Table 2 presents the yield of hydromagensite obtained in different *p*H values. From the results, it is noted that the yield increased linearly with the increase of the solution *p*H values. This may be
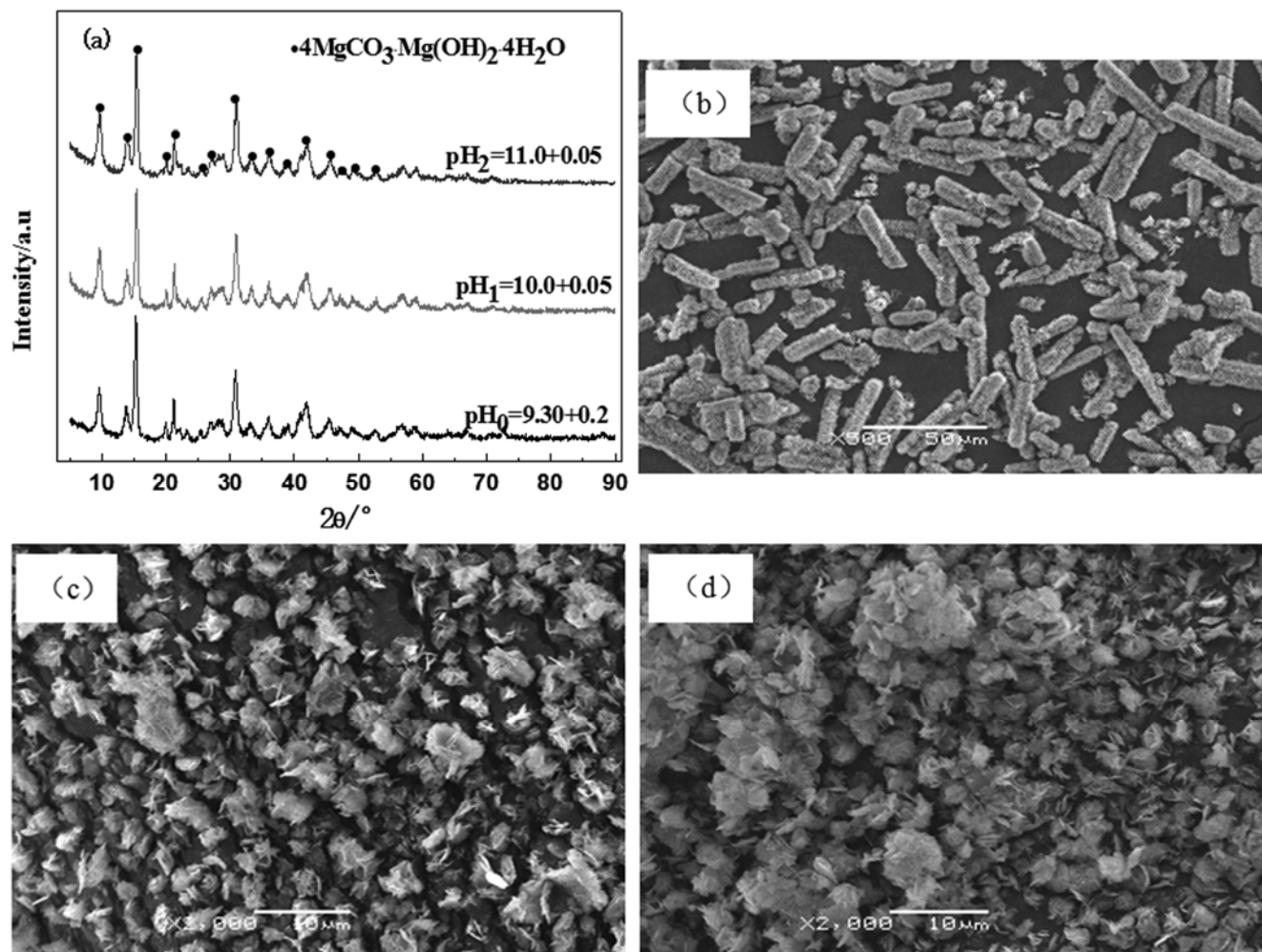

Fig. 2 — XRD patterns of products obtained with different pH values of nesquehonite solutions at 343K (a) and SEM images of products obtained with *p*H values of (b) 9.30+0.2; (c)10.0+0.05 and (d)11.0+0.05.

attributed to the OH⁻ ion concentration, which was elevated with increasing of the *p*H values. The OH⁻ ion has the most ability to promote the formation of hydromagnesite.

Effect of pyrolysis time

Figure 3 shows the XRD patterns of products prepared in different pyrolysis time. As presented in Fig. 3, when the pyrolysis time is 10min, the two magnesium carbonates (nesquehonite and hydromagnesite) were found in the obtained product. As the pyrolysis time increases to 30 min，the peaks of nesquehonite disappear and all peaks of products basically belong to hydromagnesite. When the pyrolysis time further extends to 60 min or even to 120 min, all peaks of the resultant products belong to hydromagnesite. The smooth baseline, the strong intensity of the peaks, and the narrow peak width indicate that hydromagnesite is well crystallized. The SEM images of as-synthesized samples are given in Fig. 4. It can be seen that rod-like crystals with smooth

surface, porous rod-like, and flower-like crystals are observed in 10min (Fig.4(a)). From the analysis here, it is noted that the initial phase transformed from nesquehonite to hydromagnesite when the pyrogenation time reached to 10 min. Therefore, the low purity of products was due to the incomplete phase transformation. As shown in Fig. 4(b), there are plenty of porous rod-like hydromagnesite crystals in products. It demonstrates that the phase transformations from nesquehonite to hydromagnesite was completed when the pyrogenation time reached 30 min, although the
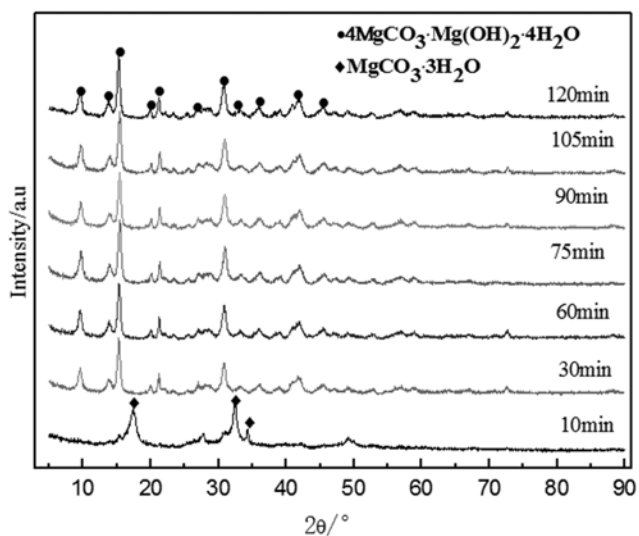
Table 2 — Yield of hydromagnesite obtained at different *p*H values of nesquehonite solutions

pH values	Mass of N, g	Theoreticla yield of H, g	Real production of H, g	Yield, %
		Results		
9.30±0.2	10.01	6.76	6.05	89.44
10.0±0.05	10.02	6.76	6.19	91.57
11.0±0.05	10.01	6.76	6.34	93.79

Fig. 3 — XRD patterns of products obtained at 343K with different reactive times
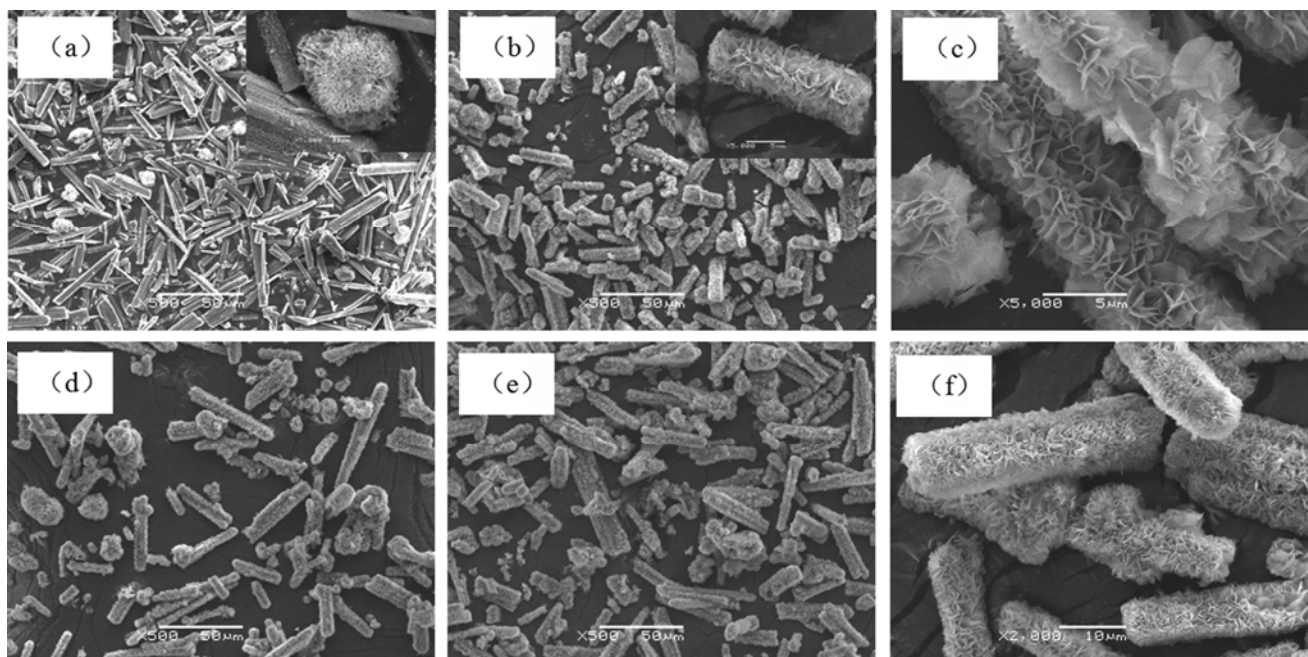

Fig. 4 — Effect of reactive times on the morphology of the products at 343k. (a)10 min; (b)30 min; (c)60 min; (d)75 min; (e)90 min and (f)120 min.

morphologies of hydromagnesite were not uniform. From the Fig. 4(c), the products are all porous rod-like hydromanesite crystals with good crystalline and uniform morphology when the pyrolysis time is 60 min. Furthermore, the pyrolysis time shows no influence on the composition and morphology of products when it is longer than 60 min (Figs 4(d), 4(e) and 4(f)).

Mechanism analysis

Phase transition kinetics can be useful in investigating the mechanism of the transition from nesquehonite to hydromagnesite. In order to analysis the phase transfer kinetics of nesquehonite, activation energy barrier (E_a), which had to be overcome during crystallization process at different pyrolysis temperatures, should be calculated. E_a used in this calculation was evaluated in accordance with the Arrhenius equation mentioned [Eq.(3)~(4)].
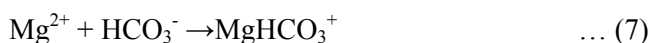
$$k = k_0 \exp(- E_a/RT) \qquad \dots (3)$$

$$\ln k = \ln k_0 - E_a / RT \qquad \dots (4)$$

where k ($mol^{-1} \cdot L \cdot min^{-1}$) is the rate constant for the phase transition kinetics, k_0 ($mol^{-1} \cdot L \cdot min^{-1}$) is the temperature-independent Arrhenius factor, E_a (kJ/mol) is the activation energy, R (8.314J/mol K) is the gas constant, and the T (K) is the temperature. The activation energy could be determined from the slope of the plot of ln$k$ versus $1/T$.

During the process of phase transition, the concentration of nesquehonite solution changed with time. To monitor the process, a conductivity measurer was used to measure the change of the solution over time. Thus, rate constant k can be calculated by electrical conductivity method.

According to above discussion, in nesquehonite aqueous systems, two types of reaction occur: dissolution of nesquehonite and association (speciation) of ionic species. The associated Mg-bearing species, *i.e.* $MgCO_3^0$, $MgHCO_3^+$, and $MgOH^+$, form during the pyrolysis process, as well as CO_3^{2-}, H^+, OH^-. The solution conductivity is governed by the equilibrium reactions (5)~(8).

$$MgCO_3 \cdot 3H_2O \rightarrow Mg^{2+} + CO_3^{2-} + 3H_2O \qquad \dots (5)$$

$$Mg^{2+} + CO_3^{2-} \rightarrow MgCO_3^0 \qquad \dots (6)$$

$$Mg^{2+} + HCO_3^- \rightarrow MgHCO_3^+ \qquad \dots (7)$$

$$Mg^{2+} + OH^- \rightarrow MgOH^+ \qquad \dots (8)$$

All above ions are capable of reacting to form precipitates, $4MgCO_3 \cdot Mg(OH)_2 \cdot 4H_2O$ Consequently, the ions of the solution were decreasing during the pyrolysis process. With the reducing of the ions, the conductivity value of the solution might decrease. The relationship between conductivity value and reaction rate constant k is expressed in [Eq.(9)].

$$\frac{1}{c} \frac{G_0 - G_t}{G_t - G_\infty} = kt \qquad \dots (9)$$

where, c is initial solution concentration, 0.2523mol/L, t is reactive time, G_0 ($ms \cdot cm^{-1}$) is the solution conductivity value when the reaction starts, G_t ($ms \cdot cm^{-1}$) is the solution conductivity value when the reactive time is equal to t, G_∞ ($ms \cdot cm^{-1}$) is the solution conductivity value when the reaction ends. Assuming that the reactive time and terminal reaction time is 60 min and 120 min, the parameters of G_0, G_{60}, G_{120} were determined，respectively. Then the parameters were put into the equation (9). Table 3 represents the conductivity and reaction rate at different temperatures and reactive time during the reaction. According to the results in Table 3, the relationship between ln$k$ and 1/T was y=3.26026-409.50165x (Fig. 5). The coefficient of fitting degree is 0.9671. It is well demonstrated that the crystallization kinetics model can effectively fit the phase transfer process of nesquehonite. The activation energy is found to be 3.4080kJ/mol (R^2=0.9671). According to Ostwald grading rules, the phase transfer rate is accelerated with the increase of temperatures. The reasons may be that nesquehonite becomes extremely unstable at high temperature[25]. The pyrolysis reaction of nesquehonite solution is endothermic reaction, and higher pyrolysis temperature is favorable to the positive reaction. Therefore, nesquehonite at metastable state in

Table 3 — Conductivity and reaction rate at different temperatures and times during the reaction

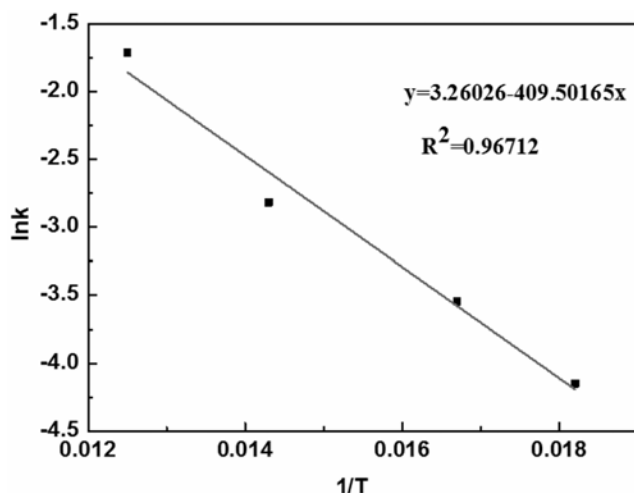| Temperature （K)	Conductivity at different times ($ms \cdot cm^{-1}$)			Rate constant k /($mol^{-1} \cdot L \cdot min^{-1}$)
	G_0	G_{60}	G_{120}	
328	3.5	3.12	1.51	0.0157
333	3.5	2.87	1.44	0.0289
343	3.5	2.48	1.37	0.0598
353	3.5	1.54	0.82	0.1796
328	3.5	3.12	1.51	0.0157

Fig. 5 — Relationship between $\ln k$ and $1/T$
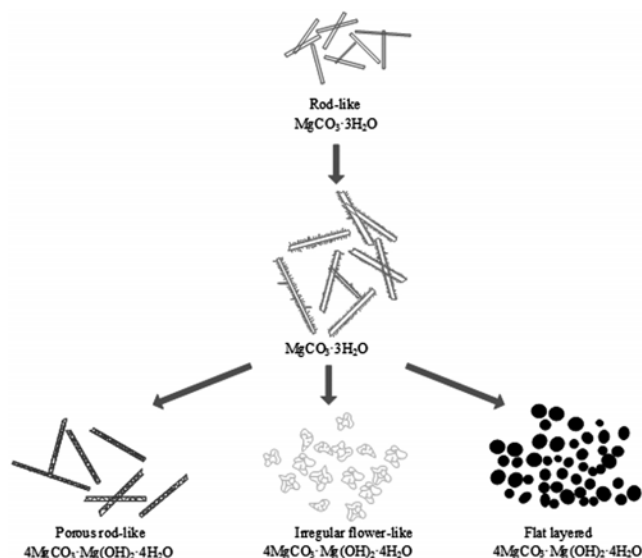
Fig. 6 — Schematic diagram of magnesium carbonate hydrate during the pyrolysis process

whiskers as raw materials. The results demonstrate that the pyrolysis temperatures and pH values place an important influence on the polymorph, morphology, and yield of products. However, the pyrolysis time shows no influence on the composition and morphology of products when it is longer than 60 min. Once the pyrolysis temperatures or pH values change, the rod-like nesquehonite can dissolve and recrystallize. Therefore, Porous rod-like, irregular flower-like and flat layered hydromagensite are eventually formed. Furthermore, the activation energy is found to be 3.4080 kJ/mol ($R^2 = 0.9671$). The results reveal that the phase transfer rate is accelerated with increasing temperatures. The kinetic analysis had good agreements with the experimental data, which suggests that the phase transfer rate is dependent on the temperature.

Acknowledgement

thermodynamics can be eventually transformed to the most stable hydromagnesite. Figure 6 shows the growth sketch map of hydromagnesite with different morphologies. It can be seen that when conditions such as pyrolysis temperature or pH value change, the surface of rod-like nesquehonite crystal will dissolve and gradually produces micro-porous and sheet structure. Porous rod-like, irregular flower-like and flat layered hydromagnesite were eventually formed.

Conclusion

The compositon and morphology of hydromagnesite is investigated by the aqueous crystallization method using self-made nesquehonite

References

1 Zamanian S & Kharat A N, Indian J Chem Technol, 23 (2016) 486.
2 Saleem R, Adnan A & Qureshi F A, *Indian J Chem Technol*, 22 (2015) 49.
3 Ding W J, Ouyang J & Yang H M. *Powder Technol*, 292 (2016) 169.
4 Chen A B, Yu Y F, Lv H J, Zhang Y, Xing T T & Yu Y H, *Mater Lett*, 135 (2014) 45.
5 Mansouri M & Atashi H, *Indian J Chem Technol*, 23 (2016) 454.
6 Song X F, Yang C, Wang J, Sun S Y & Yu JG, *Chinese J Inorg Chem*, 27 (2011) 1008.
7 Wang G S, Wang L, Cao Y & Zhang X, *Inorg Chem Ind*, 43 (2011) 31.
8 Prabhu V, Patwardha A V & Patwardhan A W, *Indian J Chem Technol*, 24 (2017) 367.
9 Narayanan S, Vijaya J J, Adinaveen T, Bououdina M & Kennedy L J, *J Nanosc Nanotechnol*, 15 (2015) 4558.
10 Wang B, Xu Z Y, Jin F, Yang J F & Ishizaki K, *Ceram Int*, 41 (2015) 5348.
11 Sun Y L, Zhao J T, Z Liu, W X Xia, Zhu S M, Lee D & Yan A R, *J Magn Magn Mater*, 379 (2015) 58.
12 Yin W Z, Wang Y L, Ji Q D, Yao J, Hou Y, Wang L & Zhong W X, *Int J Miner, Metall Mater*, 21 (2014) 305.

13 Jiang Y Z, Wang Y L, Wang C Y, Bai L M, Li X & Li Y B, *Rare Met*, 36 (2017) 997.

14 Zhu C, Wang Z R & Zhao L, *Am J Sci*, 316 (2016) 1028.

15 Zhang Z, Zheng Y, Chen J, Zhang Q, Ni Y & Liang X, *Adv Funct Mater*, 17 (2007) 2448.

16 Yang C, Song X F, Huang S S, Wang J F, Sun S Y, Sun Z & Yu J G, *Chinese J Inorg Chem*, 28 (2012) 757.

17 Yang C, Yang X B, Zheng D, Qi M J, Wang J, Song X F & Yu J G, *Inorg Chem Ind*, 43 (2011) 21.

18 Qi M J, Song X F, Yang C, Sun S Y & Yu J G, Chinese *J Inorg Chem*, 28 (2012) 1.

19 Hao Z H, Pan J & Du F L, *Mater Lett*, 63 (2009) 985.

20 Hao Z H & Du F L, *J Phys Chem Solids*, 70 (2009) 401.

21 Mitsuhashi K, Tagami N & Tanabe K. *J Photoche Photobiol A: Chem*, 185 (2007) 133.

22 Ohkubo T, Suzuki S & Mitsuhashi K, *Langmuir*, 23 (2007) 5873.

23 Cheng W T, Li Z B & George P D, *Chin J Chem Eng*, 17 (2009) 662.

24 Cheng W T & Li Z B, *Ind Eng Chem Res*, 49 (2010) 1965.

25 Wang Y & Li Z. B, *J Cryst Growth*, 310 (2008) 1224.